Cell Transplantation
2018, Vol. 27(3) 501–514

DOI: 10.1177/0963689718754561
journals.sagepub.com/home/cll
SAGE

The Route by Which Intranasally Delivered Stem Cells Enter the Central Nervous System

Carlos Galeano[1], Zhifang Qiu[1], Anuja Mishra[1], Steven L. Farnsworth[1], Jacob J. Hemmi[1], Alvaro Moreira[1], Peter Edenhoffer[1], and Peter J. Hornsby[1]

Abstract

Intranasal administration is a promising route of delivery of stem cells to the central nervous system (CNS). Reports on this mode of stem cell delivery have not yet focused on the route across the cribriform plate by which cells move from the nasal cavity into the CNS. In the current experiments, human mesenchymal stem cells (MSCs) were isolated from Wharton's jelly of umbilical cords and were labeled with extremely bright quantum dots (QDs) in order to track the cells efficiently. At 2 h after intranasal delivery in immunodeficient mice, the labeled cells were found under the olfactory epithelium, crossing the cribriform plate adjacent to the fila olfactoria, and associated with the meninges of the olfactory bulb. At all times, the cells were separate from actual nerve tracts; this location is consistent with them being in the subarachnoid space (SAS) and its extensions through the cribriform plate into the nasal mucosa. In their location under the olfactory epithelium, they appear to be within an expansion of a potential space adjacent to the turbinate bone periosteum. Therefore, intranasally administered stem cells appear to cross the olfactory epithelium, enter a space adjacent to the periosteum of the turbinate bones, and then enter the SAS via its extensions adjacent to the fila olfactoria as they cross the cribriform plate. These observations should enhance understanding of the mode by which stem cells can reach the CNS from the nasal cavity and may guide future experiments on making intranasal delivery of stem cells efficient and reproducible.

Keywords

mesenchymal stem cells, nanoparticles/nanotechnology, olfactory mucosa, Wharton's jelly, xenotransplantation, central nervous system

Introduction

The surprising observation that cells can be delivered to the central nervous system (CNS) via intranasal administration opened up the possibility that this noninvasive route could form a key part of cell therapy for neurological diseases (early work[1–6]; reviewed[7]). Since the first publication on this topic in 2009, over 40 publications have confirmed this finding and have employed several different types of stem cells, including mesenchymal stem cells (MSCs) and neural stem cells (NSCs). Cells delivered into the nasal cavity and entering the CNS appear first in the vicinity of the olfactory bulb[1–6].

In many respects, the entry of cells into the brain from the nasal cavity is unexpected, both because of the size of the agent being administered and because of the barriers that must be crossed in order for cells to enter the brain. Most other agents that can be delivered to the brain intranasally are much smaller, including a variety of small molecule drugs, proteins, viruses, and bacteria, as well as nanoparticles and microparticles[8]. Intranasally delivered agents must cross 2 substantial anatomical barriers to gain access to the brain: the olfactory epithelium and the cribriform plate. Despite the clear evidence that cells can enter the

[1] Department of Cellular and Integrative Physiology and Barshop Institute, University of Texas Health Science Center, San Antonio, TX, USA

Submitted: September 17, 2017. Revised: November 16, 2017. Accepted: December 8, 2017.

Corresponding Author:
Peter J. Hornsby, Department of Cellular and Integrative Physiology and Barshop Institute, University of Texas Health Science Center, 15355 Lambda Drive, San Antonio, TX 78245, USA.
Email: hornsby@uthscsa.edu

CNS following intranasal delivery, there is little evidence on how cells cross these barriers. Among the approximately 40 publications, only the first identified intranasally administered cells in the vicinity of the cribriform plate[1]. In that study, however, it is not clear whether cells cross the cribriform plate within the nerve tracts (fila olfactoria) or in a separate pathway.

Studies are therefore needed to address in more detail the route by which cells cross the cribriform plate to enter the brain from the nose. This is important if this route of administration is to be made more efficient and more practical. While several studies have shown efficient delivery of stem cells to the brain from the nasal cavity, some authors have stated that despite attempting to replicate experiments on nasal administration of stem cells, they found no cells crossing from the nose into the brain[9,10]. To address these issues, studies are needed to track the cells as they pass from the nasal cavity into the CNS. This is the focus of the present work.

Published data from experiments on intranasal delivery of cells need to be taken into account in considering routes and mechanisms. After cells cross the cribriform plate, they may enter the olfactory bulb and other parts of the brain via a parenchymal route or they may enter the cerebrospinal fluid (CSF), permitting movement along the surface of the cortex followed by entrance into the brain parenchyma[1]. There are therefore at least 2 routes by which cells move within the CNS after crossing the cribriform plate. Additionally, penetration of cells into the CNS from the nasal cavity is greatly enhanced by pretreatment or cotreatment of the olfactory epithelium with hyaluronidase[1–6]. It is possible that hyaluronidase acts in its classically described role as "spreading factor" that has been extensively employed in drug delivery[11], or it may act by loosening the barrier function of the olfactory epithelium;[1] it might also be absorbed across the olfactory epithelium and affect cell migration both within and beyond the nasal cavity. Moreover, penetration of cells into the CNS is very rapid, occurring within 2 h of cell delivery into the nasal cavity[1–6]. Even at 1 h after intranasal administration, numerous cells are found in the subarachnoid space (SAS), in the olfactory bulbs, and in other areas of the brain[1]. Further movement to other parts of the CNS occurs more slowly but nevertheless occurs within hours, rather than days or longer[1–6]. Damage within the CNS affects the final location of intranasally administered cells, suggesting that at least some cell types may be able to respond to cues that originate in sites of damage[12]. Multiple cell types (MSCs, macrophages, and glia, among others) have been shown to enter the CNS when delivered intranasally[13].

Considering the routes by which cells may travel from the nasal cavity to the CNS, it has been known for over a century that there is a bidirectional connection between these organs (recently reviewed[14–16]). Depending on the agent and the direction of movement (nasal cavity to CNS or CNS to nasal cavity), several different pathways across the cribriform plate have been proposed[8,14–16]. Drugs and many other materials delivered intranasally often reach the olfactory bulbs within minutes, before traveling to other parts of the brain[8]. Conversely, it has been well established that CSF exits from the cranium via the cribriform plate and enters the nasal mucosa and nasal lymphatics; this is part of the normal process of secretion and absorption of CSF[14–16]. An area of controversy has been whether substances entering the brain from the nasal cavity do so by following the route of CSF flow "upstream"; if so, it has not been explained how agents can move against the normal direction of flow of the CSF.

The cribriform plate, which separates the nasal cavity from the olfactory bulbs, forms an obvious anatomical barrier that cells or other materials must cross to enter the brain. While there does not appear to be any physiological trafficking of endogenous cells across the cribriform plate from the nasal cavity to the CNS, trafficking of cells in the reverse direction (from the CNS to the tissues of the nasal cavity) is a normal function of the immune system[17–19]. T cells and monocytes pass through the cribriform plate from the CNS to the nasal lymphatic vessels and then to the deep cervical lymph nodes. This immune cell trafficking is believed to be involved in the immune protection of the CNS. Histological studies show immune cells within the cribriform plate, adjacent to the olfactory nerves (fila olfactoria), but not closely associated with the nerve tracts[20,21]. Therefore, the pathway of exit of immune cells from the CNS may be similar to the pathway of exit of CSF[14–16]. Materials introduced into the CSF, such as India ink particles, exit via the extensions of the SAS that accompany the fila olfactoria through the cribriform plate[22–26]. Despite the fact that immune cells reach nasal lymphatic vessels, the current consensus is that there is no direct connection between these SAS extensions and lymphatics; rather, CSF and cells exit from these extensions into the submucosal tissue and from there reach lymphatics[17–19]. Although it is also known that lymphatic vessels in the dura of the CNS exit the skull base and thereby enable CSF and immune cells to reach deep cervical lymph nodes, this route is separate from the SAS/cribriform plate/nasal mucosa route[17–19]. One possibility, therefore, is that, to some extent, intranasally delivered stem cells follow the reverse of the route used by immune cells. The relevant anatomy of the nasal cavity and its connections to the CNS is reviewed in Fig. 1.

In the present experiments, we investigated the pathway across the cribriform plate by which intranasally delivered stem cells may enter the CNS, using a method that labels cells with extremely bright fluorescent nanoparticles. We used human MSCs because many of the published reports in intranasal delivery used these cells and because they are very promising with respect to their therapeutic potential[27,28]. While they are multipotent cells that can differentiate into multiple lineages, they also exert effects on tissue repair and immune modulation independent of differentiation[27,28]. Moreover, they can be derived from many tissue sources including bone marrow, fat, and Wharton's jelly of the umbilical cord[29]. MSCs have shown numerous significant effects on CNS function following intranasal administration[1,2,5,7–9].

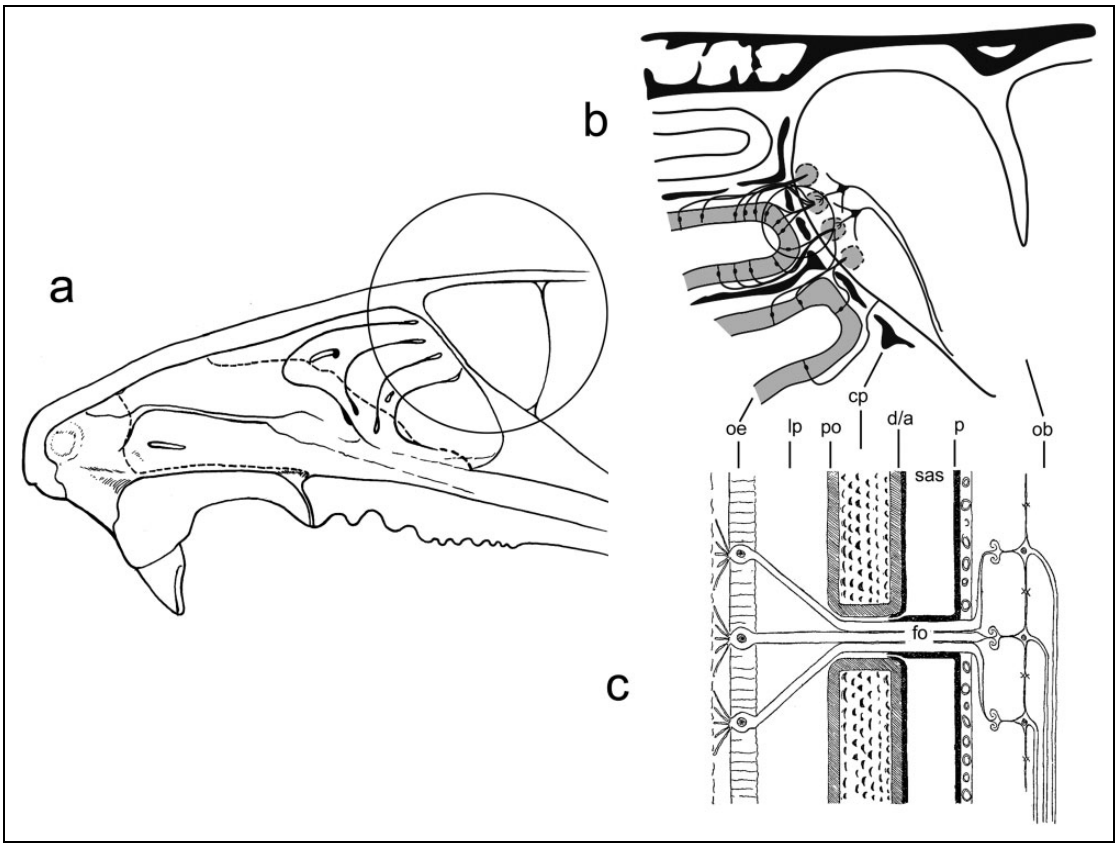

Fig. 1. The anatomy of the nasal cavity in relation to the brain. (a) Cross section of the rodent nasal cavity. The circled area is expanded in (b). (b) The communication by the olfactory nerves between the olfactory epithelium and the olfactory bulb of the brain, with the cribriform plate portion of the ethmoid bone of the skull intervening. Individual olfactory nerve cells are shown originating in the olfactory epithelium and terminating in the glomerular layer of the olfactory bulb. Bundles of axons (fila olfactoria [fo]) cross the cribriform plate. The circled area is expanded in (c). (c) Diagrammatic representation of the relationship of the subarachnoid space (SAS) and the associated dura/arachnoid (d/a) and pia mater (p) with the cribriform plate (cp) and its associated periosteum (po), the olfactory epithelium (oe) with the underlying lamina propria (lp), and the olfactory bulb (ob). The connection between the SAS and the nasal mucosa is shown here as a channel formed as an extension of the SAS into the cribriform plate ending somewhere within the lamina propria on the other side; however, the nature of these channels remains unclear as explained in the text.

Materials and Methods

Isolation and Growth of Human MSCs

MSCs were prepared from Wharton's jelly of umbilical cords[30]. The research use of human umbilical cords was approved by the institutional review board at the University of Texas Health Science Center and University Health System, San Antonio. Umbilical cords were obtained from healthy term newborns after delivery. A longitudinal incision was made to permit the removal of umbilical cord vessels. Wharton's jelly was collected and placed in 125 U/mL collagenase type I (cat. # C0130, Sigma-Aldrich, St Louis, MO, USA) in cell culture medium. The mixture was incubated at 37 °C. After 3 h, 150 μg/mL hyaluronidase type I-S (cat. # H3506, Sigma-Aldrich) was added. After a further 1 h incubation, the digested cells were collected in a 15-mL conical tube and centrifuged at 1,000 rpm for 4 min. The cell pellet was resuspended in cell culture medium and plated. The medium used was StemXVivo (cat. # CCM004, R&D Systems, Minneapolis, MN, USA) with 10% fetal bovine serum (ThermoFisher Scientific, Waltham, MA, USA). The cell population was expanded in this medium and was used for intranasal cell delivery experiments at passage 2 or 3.

To characterize the cells as MSCs, we subjected the cells to flow cytometric analysis and in vitro differentiation as we have previously described[31,32]. The cells were positive for CD90, CD73, and CD105 and negative for CD11b, as expected for MSCs[33]. The ability of the cells to differentiate toward the osteogenic, adipogenic, and chondrogenic lineages was tested. The StemPro Differentiation kit (ThermoFisher) was used to differentiate cells in the osteogenic lineage (Alizarin Red S staining) and adipogenic lineage (Oil Red O staining). Mesencult animal component-free (ACF) Chondrogenic Medium (Stemcell Technologies, Vancouver, British Columbia, Canada) was used to differentiate cells in the chondrogenic lineage (Alcian Blue staining). The cells differentiated in these different lineages as expected for authentic MSCs.

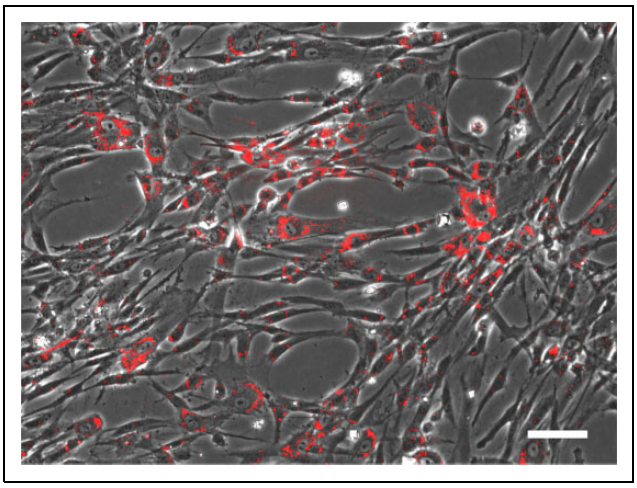

Fig. 2. Labeling of human mesenchymal stem cells (MSCs) with coated quantum dots (QDs). MSCs were isolated from Wharton's jelly of umbilical cords and were expanded in culture. Coated QDs were added to the cell culture medium as detailed in the Materials and Methods section. After 24 h, the cells were rinsed with culture medium and photographed. The image is an overlay of the phase contrast image and the fluorescence image (excitation 385 nm, emission 620 nm). Scale bar: 100 μm.

Labeling of MSCs with Coated Quantum Dots (QDs)

Coated QDs were obtained from Ocean Nanotech LLC, San Diego, CA, USA. These nanoparticles are based on cadmium selenide/zinc sulfide (CdSe/ZnS) QDs that are polymer coated and functionalized with carboxylic acid, giving a particle size of approximately 18 nm. The QDs have a 620-nm emission wavelength (catalog number QSH-620). The manufacturer states that their organic layers consist of a monolayer of oleic acid/octadecylamine and a monolayer of amphiphilic polymer. The suspension received from the manufacturer was diluted 200× in cell culture medium for addition to the cells. The medium containing the QDs was sonicated prior to addition to the cells to avoid adding aggregated QDs. Following 24 h incubation, the cells were rinsed thoroughly with culture medium (Fig. 2).

Intranasal Cell Delivery

Mice used were $Rag2^{-/-}/Il2rg^{-/-}$ (average age 6 mo); these mice are completely immunodeficient, and we have used them in numerous prior cell transplantation studies[34–36]. Although the present experiments used a maximum of 2 h following cell delivery, we used immunodeficient mice to prevent any possible immune reaction to the human MSCs. Mice were anesthetized with Avertin[37]. Although intranasal delivery does not require general anesthesia, we found it more convenient to control the administration of cells in lightly anesthetized mice (0.015 mL/g Avertin administered by intraperitoneal injection). We did not observe respiratory depression in the anesthetized animals. Labeled human MSCs were released from the culture dish with trypsin, and 300,000 cells were resuspended in 10 μL phosphate-buffered saline (PBS; with calcium and magnesium; cat. # D8662, Sigma-Aldrich) that also contained 100 U hyaluronidase type I-S (cat. # H3506, Sigma-Aldrich). The cell suspension was introduced deep into the nasal cavity using a polypropylene catheter (cat. # M-FC STD, Braintree Scientific, Braintree, MA, USA). The tip was placed far back in the nasal cavity in the region of the olfactory epithelium. The length of catheter needed to reach the olfactory epithelium was assessed by positioning the catheter in the nasal cavity of a postmortem dissected animal. The cell suspension was slowly introduced using a 10-μL glass syringe attached to the catheter. Mice were supine during this procedure and were allowed to remain in this position until they recovered from the anesthetic. At 2 h postcell delivery, mice were sacrificed using CO_2 and the entire body was cooled on ice as rapidly as possible.

Processing of Tissues for Histological Studies

For tissue processing, the nasal cavity together with the adjacent cribriform plate and olfactory bulb was dissected away from other tissues. Because of the possibility that loose cells in the nasal cavity could interfere with analysis, the nasal cavity was left intact during tissue processing and fixation. Fixation was accomplished by immersion in freshly prepared 4% paraformaldehyde[38] and subjecting the tissues to reduced pressure to remove trapped air bubbles from within the nasal cavity (reduced pressure was accomplished by placing the tissue in a vessel attached to a lyophilizer; VirTis Inc., Gardiner, NY, USA). After 24 h, the fixed tissues were placed in 14% ethylenediaminetetraacetic acid (EDTA) for decalcification of the bones of the nasal cavity, the cribriform plate, and attached portions of the skull[39]. Preliminary studies showed that acid decalcification eliminated the fluorescence of the QDs, presumably by dissolving the metal core. However, EDTA decalcification preserved fluorescence completely. The extent of decalcification was tested at 24 h intervals by flexing the bones; after 3 to 5 d, bones were soft enough to proceed with further processing.

Fixed and decalcified tissues were conventionally processed for paraffin embedding and sectioning using published protocols[38]. Sections were prepared at 10 μm thickness. QD fluorescence was easily visible following deparaffinization with xylene without further treatment. Some sections were subjected to hematoxylin and eosin staining[38].

Fluorescence Microscopy

Tissue dissection following fixation was accomplished using a stereoscopic microscope. For fluorescence photography using this microscope, a 425 nm longpass filter (Edmund Optics, Barrington, NJ, USA) was used in conjunction with illumination using a 385-nm wavelength collimated LED light source (Thor Labs, Newton, NJ, USA). Additionally, other fluorescence imaging of the intact and dissected tissues was performed using an Olympus BX50 microscope

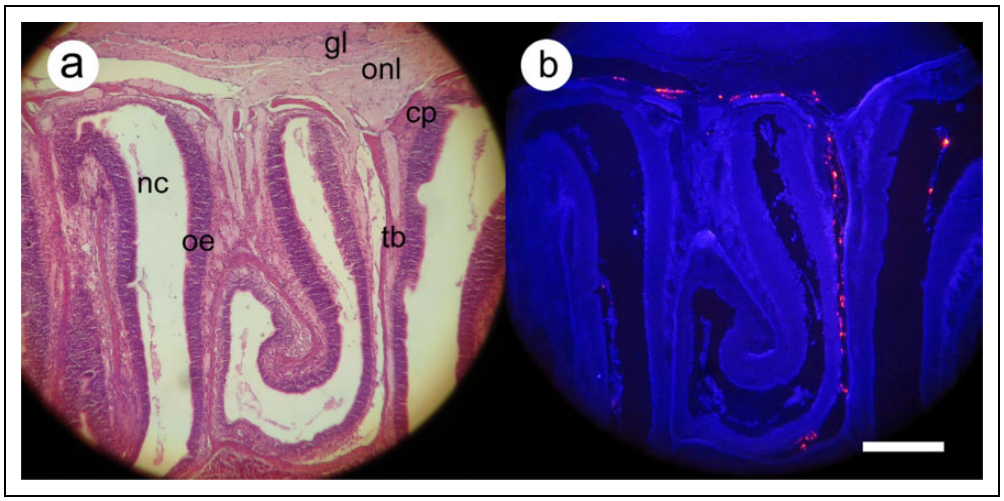

Fig. 3. Distribution of labeled mesenchymal stem cells 2 h after intranasal administration. Histological sections were processed for routine staining with hematoxylin and eosin (a) or (b) were deparaffinized only and then photographed at an excitation wavelength of 350 nm using a dual-band emission filter (see Materials and Methods section). Labeled cells appear bright red, while tissues show a dark-blue autofluorescence. Major anatomical features are marked as follows: cp, cribriform plate; nc, nasal cavity; oe, olfactory epithelium; tb, turbinate bone; within the olfactory bulb, the olfactory nerve layer (onl) and glomerular layer (gl) are indicated. Scale bar: 300 μm.

equipped with very long working distance objective lenses (Mitutoyo, Kawasaki, Japan) and adapted for fluorescence. Sections (10 μm) were photographed using a Zeiss Axiomat 200 M inverted microscope.

For both the Zeiss Axiomat and the Olympus BX50, xenon lamp illumination was used together with the following filter systems (all from Semrock Inc., Rochester, NY, USA): (1) excitation filter FF01-380/14, dichroic mirror FF409-Di03, and dual-band emission filter Em01-R405/568 (labeled cell detection); (2) same excitation filter and dichroic mirror with multiband emission filter FF01-432/515/595/730 (labeled cell detection); (3) same excitation filter and dichroic mirror with dual-band excitation filter Em01-R442/647 (used for immunohistochemistry; this filter does not permit excitation of the 620 nm QDs); and (4) same excitation filter and dichroic mirror with band-pass emission filter FF01-543/22 (used for labeled cell detection in immunohistochemistry experiments). DNA staining with YO-PRO-1 (ThermoFisher) was accomplished using the manufacturer's instructions and was photographed using a conventional fluorescein isothiocyanate filter set.

Some tissue specimens were used for confocal microscopy (Zeiss LSM 780). A 405-nm diode laser was used with detection windows of 443 to 552 nm (for imaging of the tissue background) and 605 to 633 nm (for imaging of the labeled MSCs).

Immunohistochemistry

Immunohistochemistry was performed on 10 μm sections following deparaffinization and transfer into PBS. Sections were either incubated directly with the primary antibodies or were pretreated with proteinase K for antigen retrieval[40]. Proteinase K treatment comprised a 20 min incubation at 10 μg/mL at room temperature as recommended by the manufacturer (ThermoFisher). Antibodies used were against olfactory marker protein (OMP; cat. # ab183947, Abcam Inc., Cambridge, MA, USA), fibronectin (cat. # ab2413, Abcam), and laminin (cat. # Z0097, Dako Inc., Santa Barbara, CA, USA). All were used at 1:100 dilution. Following a 1 h incubation at room temperature, sections were washed using PBS and then incubated for 1 h in appropriate biotinylated secondary antibodies. Sections were then washed again and incubated for 30 min in streptavidin–QD conjugate (cat. # Q10163MP, ThermoFisher; emission wavelength of QDs = 705 nm).

Results

Intranasal Delivery of Human MSCs

Human MSCs were prepared from Wharton's jelly of umbilical cords using enzymatic digestion and mechanical dispersion. The cell population was expanded in culture using conditions optimized for growth of human MSCs. When the cell population had expanded sufficiently, cells were labeled with coated QDs (Fig. 2). Coated QDs were chosen as the labeling agent for the following reasons: (1) preliminary studies showed that they were avidly internalized by cultured MSCs but had no toxic effects, as assessed by cell division rates (the rate of increase in cell population over several days) and migration of the cells on a cell culture plastic surface (observed by time-lapse photography: data not shown). While we found that uncoated QDs were toxic, the toxicity is entirely removed when the QDs are enclosed in polymer (see Materials and Methods section). (2) The very large Stokes shift exhibited by QDs enables sensitive detection of the cells at the emission wavelength of the QDs with

almost negligible background. Although the exciting wavelength (385 nm) produces some tissue autofluorescence, this fluorescence is at shorter wavelengths (400 to 500 nm) than the wavelength of emission of the QDs, 620 nm.

Close inspection of the cells revealed a labeling rate close to 100% (Fig. 2). Cells were introduced into the nasal cavity of mice using the procedures described in detail in the Materials and Methods section. Mice with intranasally delivered MSCs were sacrificed at 2 h postadministration. Tissues were then prepared for histological examination. The 2-h time point was selected based on published observations[1–6]. Over a period of about 2 y, approximately 60 mice were used for intranasal cell delivery. The results reported here track labeled cells within the nasal cavity, cribriform plate, and CNS. We did not attempt to count the labeled cells in various anatomical locations because we did not perform complete serial sectioning of the anatomical structures of each individual animal (nasal cavity, cribriform plate, and adjacent nervous tissue). As noted below, we encountered considerable variability in the degree to which the intranasally delivered cells were observed in the vicinity of the cribriform plate and beyond, but our focus was on examining the route taken by cells in those experiments in which cells were observed to cross the cribriform plate and enter the CNS.

Sections of tissues of the nasal cavity, together with the adjacent cribriform plate and olfactory bulb, were examined both by conventional hematoxylin/eosin staining and by fluorescence microscopy (Fig. 3). In some animals, but not all, there was clear evidence of penetration of the intranasally delivered MSCs into the nasal tissues and into the CNS. In these animals, labeled MSCs were observed in a tissue space beneath the olfactory epithelium and the lamina propria close to the turbinate bones. This space did not appear to correspond to a vessel (blood vessel or lymphatic) because it appeared in numerous consecutive sections. This observation is compatible with the cells being within an extensive sheet-like space between the epithelium and the bone, but not within a tubular structure like a vessel. At the level of the cribriform plate, cells were observed on both sides of this bone, which separates the olfactory bulb from the nasal cavity. Extensive accumulations of cells were observed on the CNS side of the cribriform plate. Based on the observation that cells are seen beneath the epithelium and on both sides of the cribriform plate, it can be inferred that cells cross the epithelium and then cross the cribriform plate into the CNS.

In order to view the distribution of cells after intranasal administration more closely, tissue sections were imaged using a different multiband filter (Fig. 4). Using this filter, the background tissue autofluorescence was brighter; this made it possible to distinguish bone, nerve, and other tissues. Nerve tracts can be seen crossing the cribriform plate. Accumulations of labeled cells can be seen on both sides of the cribriform plate, indicating that these are locations where cells cross from the nasal cavity to the olfactory bulb. Within the olfactory bulb, the different appearance of the olfactory nerve layer and the glomerular layer made it possible to conclude that cells do not penetrate into the inner portion of the olfactory bulb but remain within the outer layers of this part of the brain.

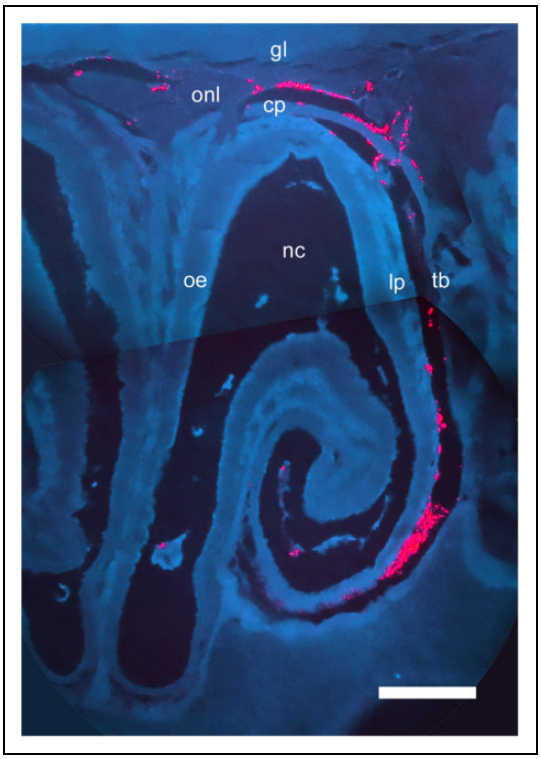

Fig. 4. Detailed examination of distribution of labeled mesenchymal stem cells 2 h after intranasal administration. In order to better observe the tissues of the nasal cavity and olfactory bulb, histological sections were photographed using 385-nm wavelength excitation and a triple-band emission filter (see Materials and Methods section). Labeled cells appear bright red. Tissues appear dark blue (autofluorescence); bone (e.g., cribriform plate [cp], turbinate bone [tb]) appears as a lighter blue than nerve tissue (e.g., within the olfactory bulb, the olfactory nerve layer [onl], and glomerular layer [gl]). Nerve fascicles are seen crossing the cribriform plate to innervate the olfactory epithelium. *Other abbreviations*: nc, nasal cavity; oe, olfactory epithelium; lp, lamina propria. Scale bar: 300 μm.

Intranasally Delivered MSCs Cross the Cribriform Plate but Remain Outside of Nerve Tracts

The preliminary conclusions from the experiments above were that intranasally delivered cells may cross the cribriform plate to the olfactory bulb but remain outside of nerve tracts, at least at this early time point (2 h postadministration). In order to further investigate these conclusions, we imaged cells crossing the cribriform plate and performed immunohistochemistry to clarify the exact locations of the cells. In Fig. 5, we show higher power images of cells crossing the cribriform plate. To positively identify cells, we used the combination of the fluorescence from the QDs combined with visualization of cell nuclei. Nuclei were identified using a DNA-binding dye. Cells, seen as nuclei surrounded by QD

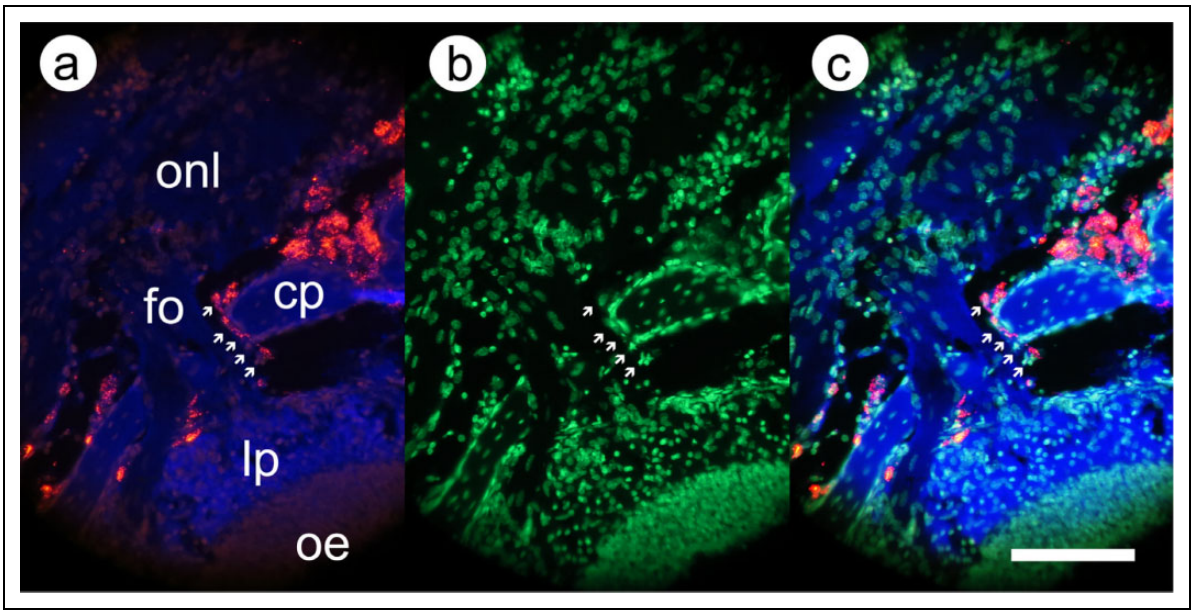

Fig. 5. Higher power images of labeled mesenchymal stem cells crossing the cribriform plate. Before photography, the deparaffinized section was incubated with YO-PRO-1 DNA-binding dye to enable visualization of cell nuclei. (a) Fluorescence image, same excitation and emission wavelengths as Fig. 3; (b) fluorescence image, excitation 480 nm and emission 530 nm (YO-PRO-1); and (c) superimposition of images from (a) and (b). Arrows indicate a series of labeled cells crossing the cribriform plate. Abbreviations as in Fig. 3; fo = fila olfactoria. Scale bar: 100 μm.

fluorescence, were observed within the cribriform plate in the gaps in the bone (foramina) that enable nerves to cross from the nasal cavity to the CNS. Cells were adjacent to nerve tracts (fila olfactoria) in the cribriform plate but not within them.

To further locate the cells on both sides of the cribriform plate, we used immunohistochemistry to (1) show nerve tracts unambiguously and (2) define the space beneath the epithelium from which cells reach the cribriform plate. In Fig. 6, sections have been stained with an antibody against OMP, which stains the olfactory nerves within the olfactory epithelium, in tracts within the lamina propria, as tracts crossing the cribriform plate, and in the olfactory nerve layer within the olfactory bulb. Labeled cells are observed in various locations on each side of the cribriform plate, but never within the nerve tracts marked by OMP. We used staining with antibodies against laminin and fibronectin to further characterize the space under the lamina propria in which the cells are located before crossing the cribriform plate. Both of these extracellular matrix proteins are constituents of the periosteum[41]. As shown in Fig. 7, the labeled cells are enmeshed in a loose tissue that stains strongly for laminin and fibronectin.

Intranasally Delivered MSCs Are Found around the Olfactory Bulb

In these studies, we tracked the intranasally delivered cells at 2 h postadministration. At this time point, based on prior studies, those cells that have entered the CNS would be expected to be in the vicinity of the olfactory bulb but not necessarily in other regions of the brain. In studies that have included time courses of distribution of the cells in the CNS, cells are found in various parts of the brain by 6 to 8 h after intranasal delivery, while at 2 h cells are predominantly in the olfactory bulb[1–6]. We verified these conclusions here by intranasal delivery of human MSCs labeled with luciferase (data not shown). When CNS tissues were extracted and assayed for luciferase activity, luciferase was easily detected in the olfactory bulb but was detectable only at much lower levels in other parts of the brain. The regions of the brain that were sampled for luciferase activity are shown in the diagram in Fig. 8. Luciferase counts were 200- to 500-fold above background in the olfactory bulbs but were 5- to 10-fold above background in the brain region adjacent to the olfactory bulb; counts in other brain regions were not above background. In a similar set of preliminary experiments performed in a small nonhuman primate, the common marmoset, we found similar results. Luciferase counts were 50- to 100-fold above background in the olfactory bulb and were not above background in the adjacent brain regions.

Based on the expectation that we could visualize the QD-labeled cells in the vicinity of the olfactory bulb, we performed imaging studies of the external olfactory bulb and the regions of the olfactory bulb close to the cribriform plate. In Fig. 9, we show that the meninges of the olfactory bulb can be identified by the presence of melanocytes as previously documented[39]. We observed melanocytes on top of the olfactory bulb and between the 2 olfactory bulbs, a region where there is an expansion of the meninges[42,43]. Labeled MSCs are seen on the upper surface of the olfactory bulb,

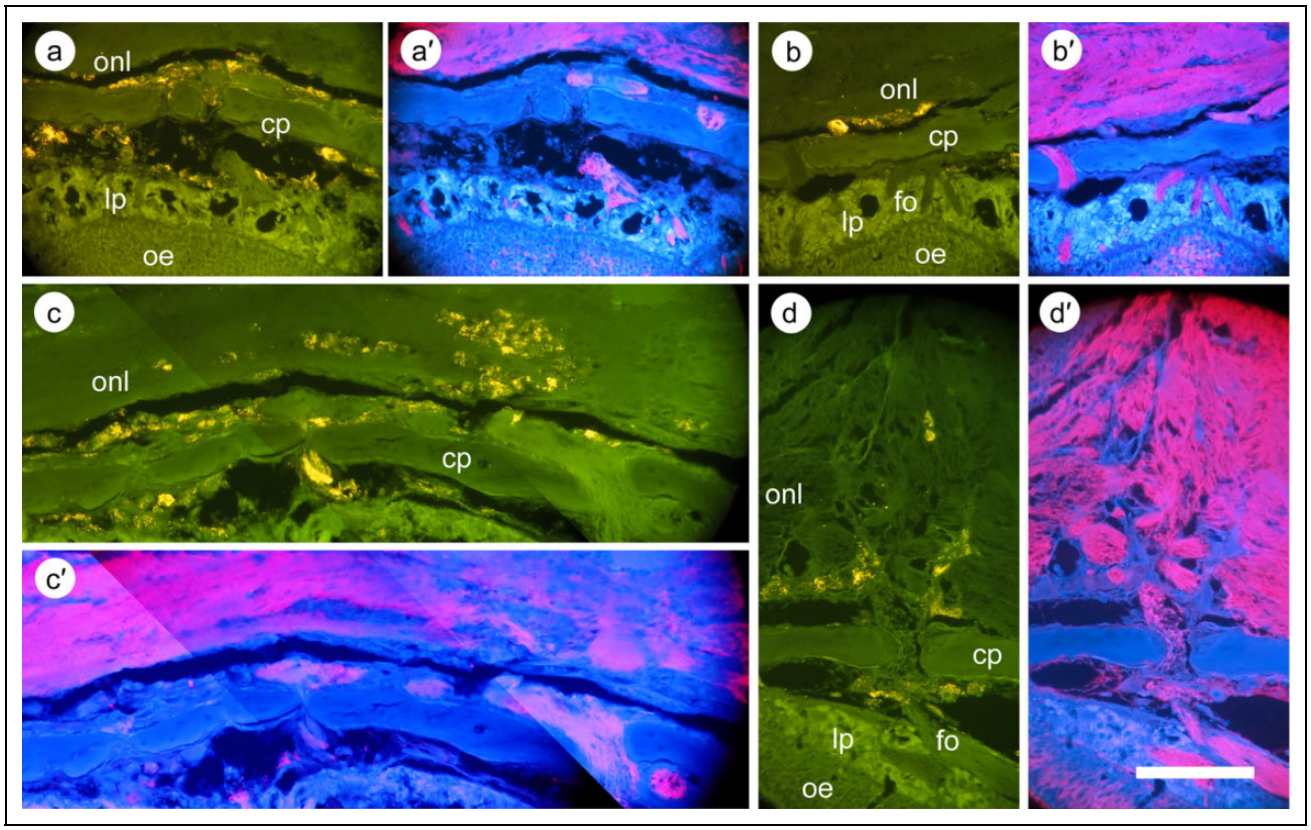

Fig. 6. Immunohistochemistry of the region of the cribriform plate and olfactory nerve layer following transplantation of labeled mesenchymal stem cells. Following sectioning of the tissue and deparaffinization, sections were incubated with an antibody against olfactory marker protein (OMP). Staining was visualized using 705-nm quantum dots (QDs; see Materials and Methods section). In order to visualize immunohistochemical staining and the labeled cell fluorescence without interference, antibody staining was observed with excitation wavelength 385 nm and emission 705 nm, while labeled cells were visualized with emission at 543 nm (cells appear yellow in the photograph). This is a suboptimal wavelength for observing the 620-nm coated QDs, but their brightness enables them to be easily visualized at this wavelength. (a)–(d) Different regions of the cribriform plate and the olfactory nerve layer; (a′)–(d′) the corresponding OMP staining. (a) Cells within and beyond the cribriform plate; in all cases, the cells are not within nerve tracts. (b) Cells behind the cribriform plate, again separate from the olfactory nerve layer. (c) Cells deeper within the olfactory nerve layer, but separate from the nerve tracts. (d) Cells farther from the cribriform plate, again among the nerve tracts, but not within them. Scale bar: 300 μm.

presumably in the meninges, and in the region of the meninges between the 2 olfactory bulbs.

We further investigated the localization of the cells between the olfactory bulbs using confocal microscopy (Fig. 8). Optical sectioning in the confocal microscope showed that the labeled cells are above the level of the cribriform plate to various extents, but accumulated in a vertical plane that corresponds to the tissue between the olfactory bulbs.

Many Intranasally Delivered MSCs Remain within the Nasal Cavity

We noted a great deal of variability among different experiments in the number of cells that crossed the cribriform plate. However, we also observed that it was possible to reproducibly place large numbers of cells into the part of the nasal cavity that is adjacent to the cribriform plate; therefore, the variability among experiments is not due to failure to deliver the cells to the proper location in the nasal cavity but results from unknown factors that cause variability in the number that cross the cribriform plate as discussed further below. Figure 10 shows the delivery of cells to the appropriate location in the nasal cavity. The QD-labeled cells are so brightly fluorescent that they can be observed in a distinct pattern beneath the cribriform plate (Fig. 10b). Figure 10a shows that the mouse cribriform plate is a very thin, transparent bone. Cells delivered to the nasal cavity can be seen in a pattern that corresponds to the blind ends of the ethmoturbinates[44,45]. In order to demonstrate that the cells are beneath the cribriform plate but have not penetrated it, we dissected the cribriform plate and released the cells (Fig. 10d). Cells were released as a cylindrical mass when the cribriform plate was broken in the vicinity of the accumulated cells.

Discussion

Intranasal administration is an increasingly employed mode of delivery of many therapeutic agents for treatment of CNS disorders[46]. The demonstration that cells may be delivered to

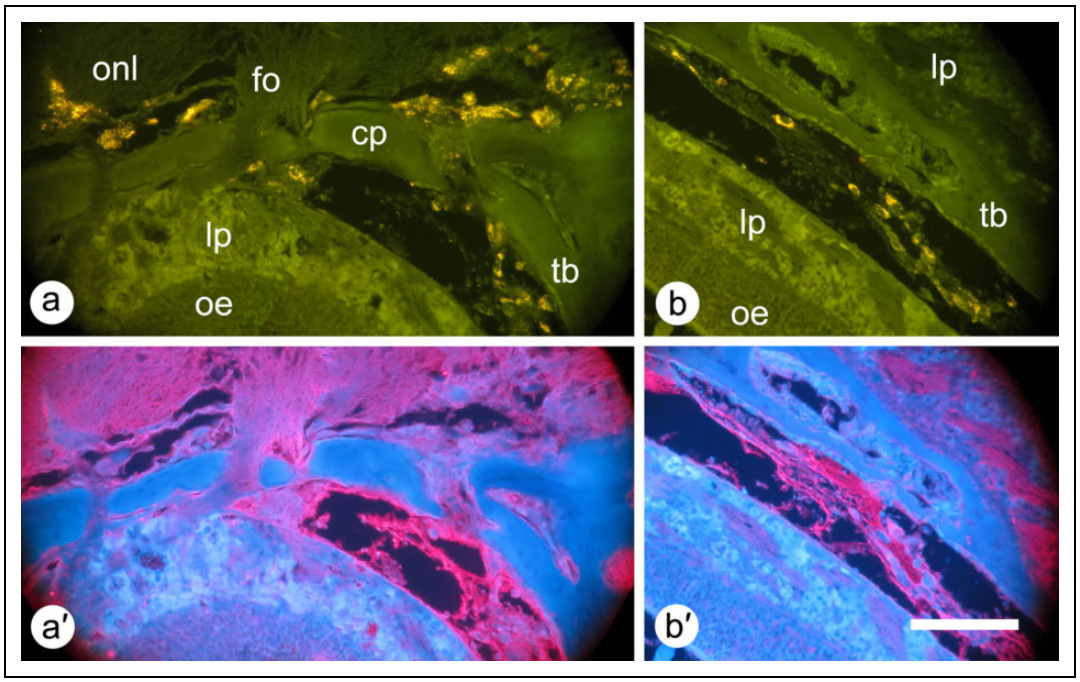

Fig. 7. Immunohistochemistry of the cribriform plate and the space beneath the turbinate bone (a) and the same space farther away from the cribriform plate (b). The sections were stained using antibodies against laminin (a) and fibronectin (b) using the same methods described in Fig. 6. (a) Cells on either side of the cribriform plate. Cells on the nasal cavity side of the cribriform plate are enmeshed in loose tissue staining strongly for laminin. (b) Cells in the space adjacent to the turbinate bone, again enmeshed in loose tissue, staining for fibronectin. Scale bar: 300 μm.

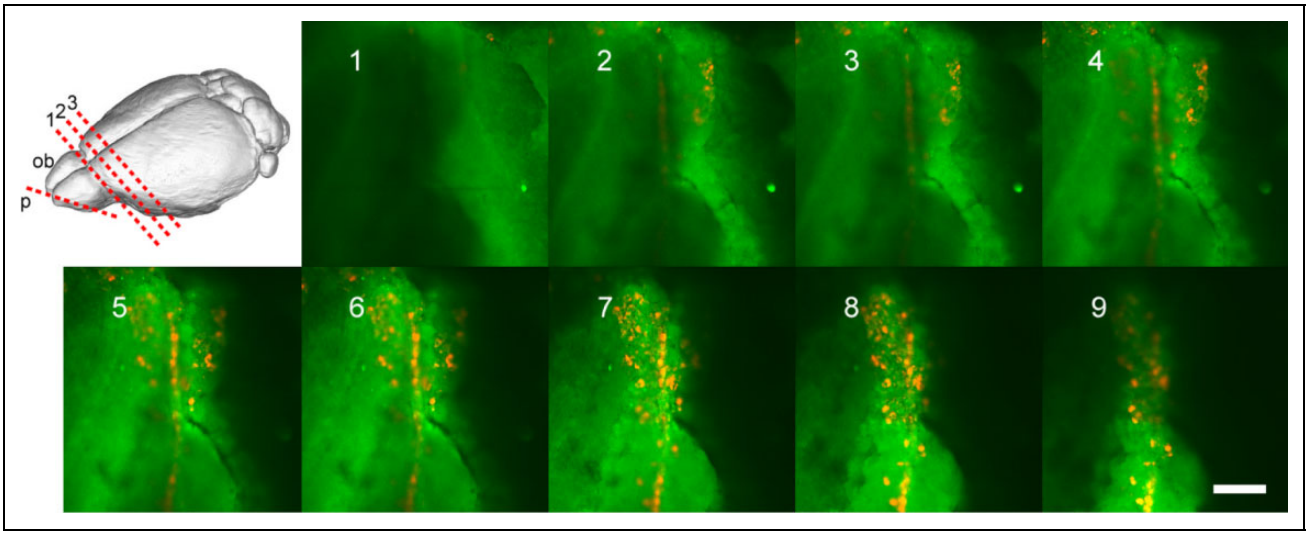

Fig. 8. Confocal microscope imaging of labeled mesenchymal stem cells (MSCs) within the olfactory bulb. The cribriform plate with attached olfactory bulb tissue (about 2 mm thick) was used for confocal microscopy. The optical plane of focus (p) is indicated in red in the upper-left image; additionally, 1, 2, and 3 indicate the cuts used to isolate the olfactory bulb tissue and the 2 adjacent brain regions for luciferase measurements (see text). Photos 1 through 9 are of descending planes of focus moving down through the olfactory bulb toward the cribriform plate. A 405-nm diode laser was used with detection windows of 443 to 552 nm (for imaging of the tissue background) and 605 to 633 nm (for imaging of the labeled MSCs). Scale bar: 250 μm.

the CNS intranasally, while relatively recent, followed more than 100 years of studies on the anatomical and functional links between the nose and the brain[14–16]. Many drugs, vaccines, and so on, are routinely delivered intranasally[8]. Moreover, many pathogens enter the body via the nose and some of these enter the CNS via this route including viruses, bacteria, and a few eukaryotes[47]. Considering the large body of literature on the anatomical nature of the connection between the nasal cavity and the brain, the finding that stem cells can enter the brain from the nose was unexpected.

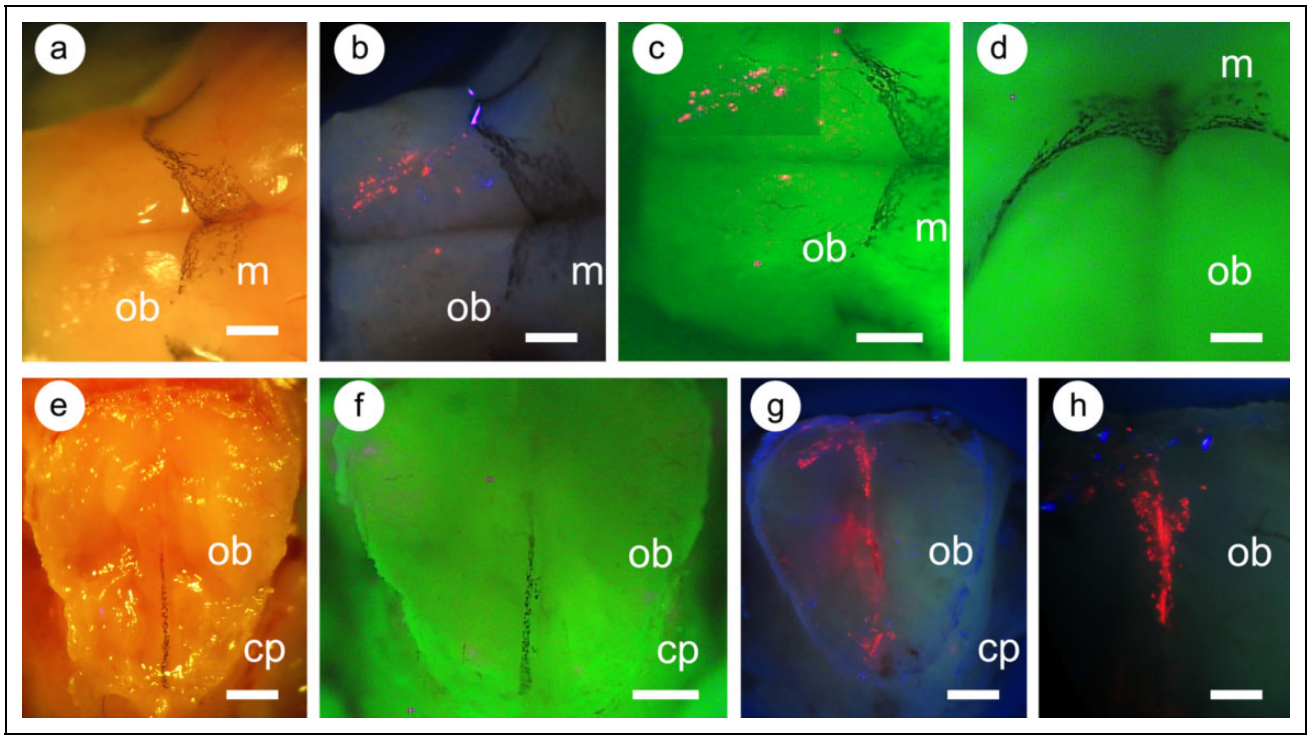

Fig. 9. Distribution of labeled mesenchymal stem cells (MSCs) in the region of the olfactory bulb following intranasal administration. The olfactory bulb and attached cribriform plate were dissected from mice 2 h following administration of labeled MSCs. The olfactory bulb (a to d) and cribriform plate with attached olfactory bulb tissue (e to h) were photographed. (a) and (e) Normal white-light illumination; (b), (g), and (h) excitation at 385 nm, photographed using a longpass filter (>400 nm); and (c), (d), and (f) 385 nm illumination and multiband filter emission. The olfactory bulbs (ob) are indicated; the associated meninges (m) are visible due to the presence of melanocytes. (d) An oblique view of meningeal melanocytes; (f) Melanocytes in the meningeal layers between the olfactory bulbs. Labeled cells appear red. In (e) to (h), the edge of the cribriform plate (cp) is seen next to the remaining olfactory bulb tissue (about 2 mm thick). Scale bars: 1 mm (a to c), 500 μm (d), and 250 μm (e to h).

Apart from a few eukaryote pathogens, entry into the brain from the nose has been demonstrated only for molecules or agents no bigger than microparticles. The route by which intranasally delivered cells can cross the cribriform plate to enter the brain from the nose is not clear from the literature and has not been a specific focus of published experiments.

In the present experiments, we delivered human MSCs intranasally to immunodeficient mice. Although an acute immune reaction to human cells may be unlikely, we chose to use an immunodeficient model in order to avoid the complications of any such reaction[48]. We found that intranasally delivered human MSCs are observed beneath the nasal mucosa, in a space next to the turbinate bones, and can be observed traveling through the cribriform plate. They are not closely associated with nerve tracts at any location including within the lamina propria, the cribriform plate, or on the CNS side of the cribriform plate. Once across the cribriform plate, cells are observed within the olfactory nerve layer and associated with the meninges around the olfactory bulbs. In both of these locations, it is likely that cells are within the major meningeal space, the SAS (Fig. 1).

The new observation on the route from the nasal cavity to the CNS is that cells are found in a space next to the turbinate bones beneath the lamina propria. Previous studies have shown that cells move en masse, relatively rapidly, from the nasal cavity to the CNS, yet there is no obvious anatomical route open for this movement. One possible route would be a reversal of that taken by immune cells trafficking from the CNS to the deep cervical lymph nodes. In that case, it has been shown that cells enter the lymphatics of the nasal tissues after moving through the cribriform plate[17–19]. However, it would be unlikely that intranasally delivered cells could travel in a reversal of this route to enter the CNS from the nose for 2 reasons. First, there is no obvious route from the outside of the olfactory epithelium to reach the inside of the lymphatic vessels; second, even if they entered lymphatics, cells would appear to be subject to being swept into the deep cervical lymph nodes by the direction of flow within these vessels.

Given that there is no obvious route by which cells could enter the brain from the nose, it is perhaps therefore not so surprising that we found that cells appear to move along a space that becomes available next to the turbinate bones, extending to the cribriform plate. This is a space between the periosteum and the lamina propria or possibly within the periosteum itself. Presumably, this is a potential space and not one that exists in the living animal. However, the same

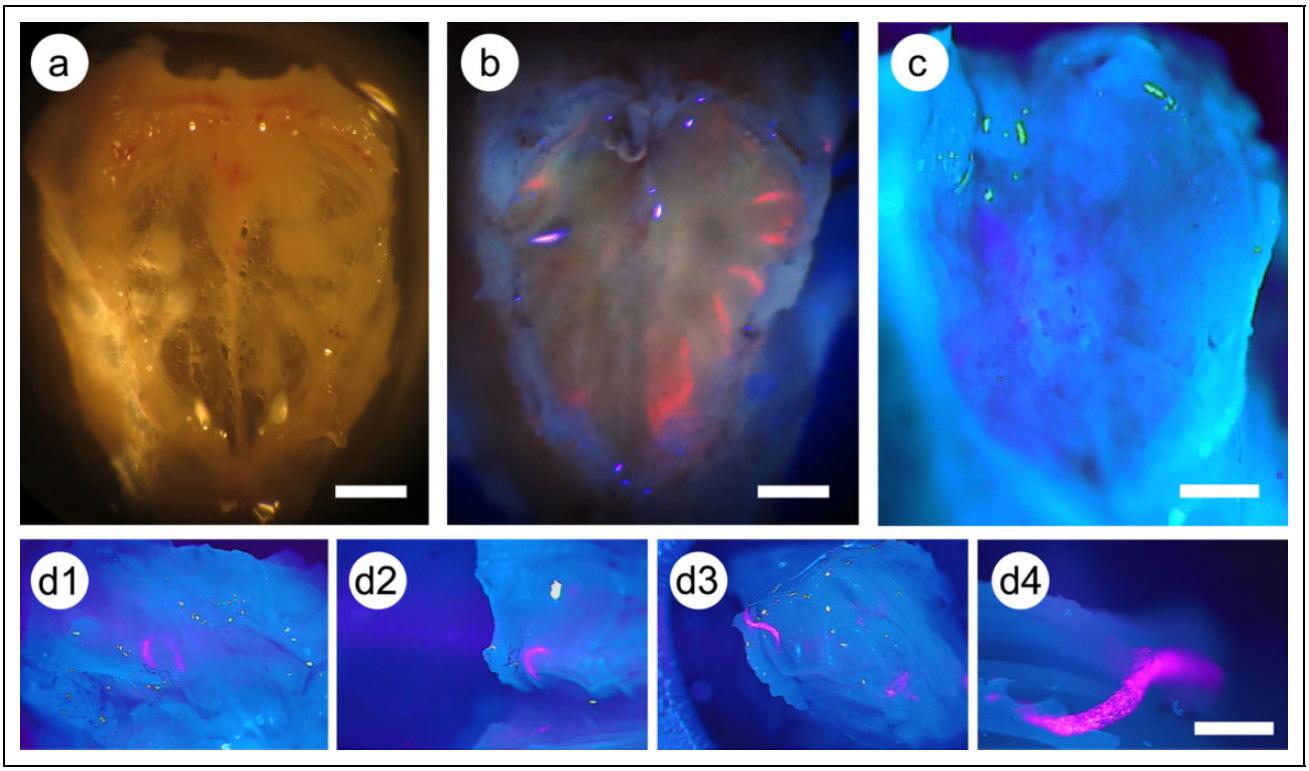

Fig. 10. Labeled mesenchymal stem cells (MSCs) beneath the cribriform plate in the nasal cavity. (a) Cribriform plate that has been isolated and cleaned of adherent tissue; normal white-light illumination. (b) Mouse received labeled MSCs intranasally and was sacrificed after 2 h; preparation comprising the nasal cavity (not dissected), cribriform plate, and attached thin layer of olfactory bulb. Photographed with 385 nm excitation and longpass filter (>400 nm). (c) and (d1 to d4) Cribriform plate preparations photographed with 385 nm excitation and dual wavelength excitation filter. (c) The general morphology of the cribriform plate using this form of microscopy. (d1 to d4) A part of a cribriform plate preparation, with underlying nasal cavity as in (b). The plate was dissected to release the underlying cells from the nasal cavity. As shown in (d4), the cells form a tight-packed mass, most of which remain in the nasal cavity and do not cross the cribriform plate. Scale bars: 250 μm.

location is well known to be the site of formation of a hematoma or abscess following trauma[49]. In contexts other than trauma, this potential space has received little attention. Nevertheless, agents administered intranasally or into the SAS can be observed accumulating in this location, possibly being passively trapped in this anatomical site. In 1929, Wilfrid le Gros Clark described experiments in which rabbits were given Prussian Blue dye intranasally and reported the results as follows: "Periosteum and Perichondrium. There is a marked tendency for the blue granules [Prussian Blue dye] to appear infiltrating the periosteum and perichondrium covering the skeletal turbinate system. The granules here do not lie in vessels but in among the cellular tissue spaces"[50(p. 18)]. Similar observations were made in other early work[51,52]. More recently, in an EM study of the route by which India ink particles reach the nasal cavity after administration into the SAS, cleft-like spaces were sometimes observed between the periosteum and the perineurium of adjacent olfactory nerves. Ink particles were observed in this space[26].

Nevertheless, the direction of movement of intranasally administered cells is surprising in view of the fact that there is a normal exit of CSF from the CNS via the cribriform plate into the nasal cavity. Elevated intracranial pressure may even cause rhinorrhea, a continuous leakage of large amounts of CSF through the cribriform plate, the fluid exiting through the nose[53]. Intracranial fluid pressure can also be negative in both experimental animals and human subjects[54], but this has not been associated with a backflow of fluid from the nasal cavity into the CNS. It has been suggested that a negative pressure gradient collapses the perineural space around the olfactory nerves as they cross the cribriform plate and thereby acts as a one-way valve[55]. Presumably, under conditions in which cells pass from the nasal cavity to the CNS, an anatomical route has opened up and the normal limitations on the passage of material from nose to CNS have been overcome. The circumstances under which this happens are not clear; they may involve specific pressure gradients between the nasal cavity and the CNS or may depend on alterations in tissue structure, such as the opening up of a space at the surface of the periosteum. Greater understanding of the nature of these factors that permit movement of cells from nasal cavity to CNS would assist in defining conditions that make intranasal cell administration more reproducible and efficient.

While the cribriform plate forms a notable barrier to the entry of intranasally administered agents into the CNS, the

olfactory epithelium comprises an equally substantial barrier to CNS entry. Nevertheless, it has been known for over a century that many materials can cross the epithelium when administered intranasally. There may be multiple mechanisms by which materials can cross: many small molecules cross via paracellular and transcellular mechanisms, but, remarkably, much larger materials have been well documented to be able to cross the epithelium. Notably, a series of experiments investigated the entry of homogenized brain material from the nasal cavity as part of studies on infection of experimental animals with prions[56,57]. Large fragments of homogenized brain material (of the order of 100 μm) were clearly observed in various stages of traversing the epithelium. The authors report that inoculum was identified in spaces of >5 μm between a small number of cells in the epithelium in >90% of animals. This type of transport took place through preexisting spaces in the nasal mucosa that are orders of magnitude wider than expected for paracellular transport. The frequency of these breaks, and whether they are normally present or require some degree of damage to the epithelium, has not been established. It is possible therefore that these breaks enable stem cells administered into the nasal cavity to cross the epithelium.

In order for intranasal cell delivery to be clinically relevant, it must be made reproducible and efficient. The present experiments indicate the direction of possible approaches to overcome these challenges. Meanwhile, the question arises as to whether intranasal stem cell delivery is applicable to primates as well as rodents. In preliminary studies to address this, we have administered stem cells to common marmosets, using the same protocols as described for mice in these experiments. Cells were labeled with luciferase to enable detection of the administered cells. As with the current experiments in mice, luciferase was detectable in the olfactory bulbs in some animals. This provides preliminary evidence that the same route of cell delivery from nasal cavity to CNS is applicable to a nonhuman primate. Much more needs to be done before this mode of administration should be attempted in human subjects, and further experiments on nonhuman primates will be essential.

Authors' Note

Carlos Galeano and Zhifang Qiu contributed equally to this work.

Ethical Approval

The experimental protocols were approved by the institutional animal care and use committee of the University of Texas Health Science Center. The research use of human umbilical cords was approved as mentioned in the Statement of Human and Animal Rights.

Statement of Human and Animal Rights

This study was approved by the institutional review board of the University of Texas Health Science Center and informed patient consent was obtained. This study was conducted in accordance with the Guide for the Care and Use of Laboratory Animals, published by the National Institutes of Health, Bethesda, MD, USA.

Statement of Informed Consent

Informed consent for the use of human umbilical cords was obtained as described in Statement of Human and Animal Rights.

Declaration of Conflicting Interests

The author(s) declared no potential conflicts of interest with respect to the research, authorship, and/or publication of this article.

Funding

The author(s) disclosed receipt of the following financial support for the research, authorship, and/or publication of this article: This work was supported by VA Merit Grant I01 BX001454, by a grant from the Owens Medical Foundation, by grant R03 AG045481 from the National Institute on Aging, and by grant P51 OD011133 (Southwest National Primate Research Center).

References

1. Danielyan L, Schafer R, von Ameln-Mayerhofer A, Buadze M, Geisler J, Klopfer T, Burkhardt U, Proksch B, Verleysdonk S, Ayturan M, Buniatian GH, Gleiter CH, Frey WH, II. Intranasal delivery of cells to the brain. Eur J Cell Biol. 2009;88(6): 315–324.
2. van Velthoven CT, Kavelaars A, van Bel F, Heijnen CJ. Nasal administration of stem cells: a promising novel route to treat neonatal ischemic brain damage. Pediatr Res. 2010;68(5): 419–422.
3. Reitz M, Demestre M, Sedlacik J, Meissner H, Fiehler J, Kim SU, Westphal M, Schmidt NO. Intranasal delivery of neural stem/progenitor cells: a noninvasive passage to target intracerebral glioma. Stem Cells Transl Med. 2012;1(12):866–873.
4. Fransson M, Piras E, Burman J, Nilsson B, Essand M, Lu B, Harris RA, Magnusson PU, Brittebo E, Loskog AS. CAR/FoxP3-engineered T regulatory cells target the CNS and suppress EAE upon intranasal delivery. J Neuroinflammation. 2012;9:112.
5. Wei N, Yu SP, Gu X, Taylor TM, Song D, Liu XF, Wei L. Delayed intranasal delivery of hypoxic-preconditioned bone marrow mesenchymal stem cells enhanced cell homing and therapeutic benefits after ischemic stroke in mice. Cell Transplant. 2013;22(6):977–991.
6. Wu S, Li K, Yan Y, Gran B, Han Y, Zhou F, Guan YT, Rostami A, Zhang GX. Intranasal delivery of neural stem cells: a CNS-specific, non-invasive cell-based therapy for experimental autoimmune encephalomyelitis. J Clin Cell Immunol. 2013; 4(3):977–991.
7. Jiang Y, Zhu J, Xu G, Liu X. Intranasal delivery of stem cells to the brain. Expert Opin Drug Deliv. 2011;8(5):623–632.
8. Lochhead JJ, Thorne RG. Intranasal delivery of biologics to the central nervous system. Adv Drug Deliv Rev. 2012;64(7): 614–628.
9. Chartoff EH, Damez-Werno D, Sonntag KC, Hassinger L, Kaufmann DE, Peterson J, McPhie D, Cataldo AM, Cohen BM. Detection of intranasally delivered bone marrow-

derived mesenchymal stromal cells in the lesioned mouse brain: a cautionary report. Stem Cells Int. 2011;2011:586586.
10. Bossolasco P, Cova L, Levandis G, Diana V, Cerri S, Lambertenghi Deliliers G, Polli E, Silani V, Blandini F, Armentero MT. Noninvasive near-infrared live imaging of human adult mesenchymal stem cells transplanted in a rodent model of Parkinson's disease. Int J Nanomedicine. 2012;7:435–447.
11. Buhren BA, Schrumpf H, Hoff NP, Bolke E, Hilton S, Gerber PA. Hyaluronidase: from clinical applications to molecular and cellular mechanisms. Eur J Med Res. 2016;21:5.
12. Danielyan L, Schafer R, von Ameln-Mayerhofer A, Bernhard F, Verleysdonk S, Buadze M, Lourhmati A, Klopfer T, Schaumann F, Schmid B, Koehle C, Proksch B, Weissert R, Reichardt HM, van den Brandt J, Buniatian GH, Schwab M, Gleiter CH, Frey WH, II. Therapeutic efficacy of intranasally delivered mesenchymal stem cells in a rat model of Parkinson disease. Rejuvenation Res. 2011;14(1):3–16.
13. Danielyan L, Beer-Hammer S, Stolzing A, Schafer R, Siegel G, Fabian C, Kahle P, Biedermann T, Lourhmati A, Buadze M, Novakovic A, Proksch B, Gleiter CH, Frey WH, Schwab M. Intranasal delivery of bone marrow-derived mesenchymal stem cells, macrophages, and microglia to the brain in mouse models of Alzheimer's and Parkinson's disease. Cell Transplant. 2014; 23(Suppl 1): S123–S39.
14. Chen L, Elias G, Yostos MP, Stimec B, Fasel J, Murphy K. Pathways of cerebrospinal fluid outflow: a deeper understanding of resorption. Neuroradiology. 2015;57(2):139–147.
15. Miyajima M, Arai H. Evaluation of the production and absorption of cerebrospinal fluid. Neurol Med Chir (Tokyo). 2015; 55(8):647–656.
16. Coles JA, Myburgh E, Brewer JM, McMenamin PG. Where are we? The anatomy of the murine cortical meninges revisited for intravital imaging, immunology, and clearance of waste from the brain. Prog Neurobiol. 2017;156:107–148.
17. Engelhardt B, Carare RO, Bechmann I, Flugel A, Laman JD, Weller RO. Vascular, glial, and lymphatic immune gateways of the central nervous system. Acta Neuropathol. 2016;132(3): 317–338.
18. Kipnis J. Multifaceted interactions between adaptive immunity and the central nervous system. Science. 2016;353(6301): 766–771.
19. Engelhardt B, Vajkoczy P, Weller RO. The movers and shapers in immune privilege of the CNS. Nat Immunol. 2017;18(2): 123–131.
20. Goldmann J, Kwidzinski E, Brandt C, Mahlo J, Richter D, Bechmann I. T cells traffic from brain to cervical lymph nodes via the cribroid plate and the nasal mucosa. J Leukoc Biol. 2006;80(4):797–801.
21. Kaminski M, Bechmann I, Pohland M, Kiwit J, Nitsch R, Glumm J. Migration of monocytes after intracerebral injection at entorhinal cortex lesion site. J Leukoc Biol. 2012;92(1):31–39.
22. Jackson RT, Tigges J, Arnold W. Subarachnoid space of the CNS, nasal mucosa, and lymphatic system. Arch Otolaryngol. 1979;105(4):180–184.
23. Pile-Spellman JM, McKusick KA, Strauss HW, Cooney J, Taveras JM. Experimental in vivo imaging of the cranial perineural lymphatic pathway. Am J Neuroradiol. 1984;5(5): 539–545.
24. Kida S, Pantazis A, Weller RO. CSF drains directly from the subarachnoid space into nasal lymphatics in the rat. Anatomy, histology and immunological significance. Neuropathol Appl Neurobiol. 1993;19(6):480–488.
25. Moinuddin SM, Tada T. Study of cerebrospinal fluid flow dynamics in TGF-beta 1 induced chronic hydrocephalic mice. Neurol Res. 2000;22(2):215–222.
26. Walter BA, Valera VA, Takahashi S, Ushiki T. The olfactory route for cerebrospinal fluid drainage into the peripheral lymphatic system. Neuropathol Appl Neurobiol. 2006;32(4): 388–396.
27. Polymeri A, Giannobile WV, Kaigler D. Bone marrow stromal stem cells in tissue engineering and regenerative medicine. Horm Metab Res. 2016;48(11):700–713.
28. Rizk M, Aziz J, Shorr R, Allan DS. Cell-based therapy using umbilical cord blood for novel indications in regenerative therapy and immune modulation: an updated systematic scoping review of the literature. Biol Blood Marrow Transplant. 2017; 23(10):1607–1613.
29. Mitchell KE, Weiss ML, Mitchell BM, Martin P, Davis D, Morales L, Helwig B, Beerenstrauch M, Abou-Easa K, Hildreth T, Troyer D, Medicetty S. Matrix cells from Wharton's jelly form neurons and glia. Stem Cells. 2003;21(1):50–60.
30. Salehinejad P, Alitheen NB, Ali AM, Omar AR, Mohit M, Janzamin E, Samani FS, Torshizi Z, Nematollahi-Mahani SN. Comparison of different methods for the isolation of mesenchymal stem cells from human umbilical cord Wharton's jelly. In Vitro Cell Dev Biol Anim. 2012;48(2):75–83.
31. Moreira A, Kahlenberg S, Hornsby PJ. Therapeutic potential of mesenchymal stem cells for diabetes. J Mol Endocrinol. 2017; 59(3):R109–R120.
32. Moreira A, Alayli Y, Balgi S, Winter C, Kahlenberg S, Mustafa S, Hornsby PJ. Upcycling umbilical cords: bridging regenerative medicine with neonatology. J Maternal Fetal Neonatal Med. 2017:1–10.
33. Dominici M, Le Blanc K, Mueller I, Slaper-Cortenbach I, Marini F, Krause D, Deans R, Keating A, Prockop DJ, Horwitz E. Minimal criteria for defining multipotent mesenchymal stromal cells. The international society for cellular therapy position statement. Cytotherapy. 2006;8(4):315–317.
34. Huang Q, Chen M, Liang S, Acha V, Liu D, Yuan F, Hawks CL, Hornsby PJ. Improving cell therapy—experiments using a cell transplantation model in immunodeficient mice. Mech Age Dev. 2007;128(1):25–30.
35. Cardoso CC, Bornstein SR, Hornsby PJ. Optimizing orthotopic cell transplantation in the mouse adrenal gland. Cell Transplant. 2010;19(5):565–572.
36. Mishra A, Qiu Z, Farnsworth SL, Hemmi JJ, Li M, Pickering AV, Hornsby PJ. Induced pluripotent stem cells from nonhuman primates. Methods Mol Biol. 2016;1357:183–193.
37. Papaioannou VE, Fox JG. Efficacy of tribromoethanol anesthesia in mice. Lab Anim Sci. 1993;43(2):189–192.
38. Greenfield EA.Antibodies: a laboratory manual. 2nd ed. Harbor (NY): CSHL Press, Cold Spring; 2014.

39. Harris N, Carter CA, Misra M, Maronpot R. Immunohistochemistry on decalcified rat nasal cavity: trials and successes. J Histotechnol. 2013;36(3):92–99.
40. Ramos-Vara JA, Beissenherz ME. Optimization of immunohistochemical methods using two different antigen retrieval methods on formalin-fixed paraffin-embedded tissues: experience with 63 markers. J Vet Diagn Invest. 2000;12(4): 307–311.
41. Nilsson SK, Debatis ME, Dooner MS, Madri JA, Quesenberry PJ, Becker PS. Immunofluorescence characterization of key extracellular matrix proteins in murine bone marrow in situ. J Histochem Cytochem. 1998;46(3):371–377.
42. Gudjohnsen SA, Atacho DA, Gesbert F, Raposo G, Hurbain I, Larue L, Steingrimsson E, Petersen PH. Meningeal melanocytes in the mouse: distribution and dependence on *Mitf*. Front Neuroanat. 2015;9:149.
43. Bedussi B, van Lier MG, Bartstra JW, de Vos J, Siebes M, VanBavel E, Bakker EN. Clearance from the mouse brain by convection of interstitial fluid towards the ventricular system. Fluids Barriers CNS. 2015;12:23.
44. Harkema JR, Carey SA, Wagner JG, Dintzis SM, Liggitt D. Nose, sinus, pharynx, and larynx. In: Treuting PM, Dintzis SM, Frevert CW, Liggitt D, Montine KS, editors. Comparative anatomy and histology: a mouse and human atlas. Amsterdam (the Netherlands): Academic Press; 2012. p. 71–94.
45. Coppola DM, Craven BA, Seeger J, Weiler E. The effects of naris occlusion on mouse nasal turbinate development. J Exp Biol. 2014;217(Pt 12):2044–2052.
46. Chapman CD, Frey WH II, Craft S, Danielyan L, Hallschmid M, Schioth HB, Benedict C. Intranasal treatment of central nervous system dysfunction in humans. Pharm Res. 2013; 30(10):2475–2484.
47. Dando SJ, Mackay-Sim A, Norton R, Currie BJ, St John JA, Ekberg JA, Batzloff M, Ulett GC, Beacham IR. Pathogens penetrating the central nervous system: infection pathways and the cellular and molecular mechanisms of invasion. Clin Microbiol Rev. 2014;27(4):691–726.
48. Yamada K, Scalea J. Current progress in xenogeneic tolerance. Curr Opin Organ Transplant. 2012;17(2):168–173.
49. Alshaikh N, Lo S. Nasal septal abscess in children: from diagnosis to management and prevention. Int J Pediatr Otorhinolaryngol. 2011;75(6):737–744.
50. le Gros Clark WE. Report of the committee on vaccination on an anatomical investigation into the routes by which infections may pass from the nasal cavities into the brain. Reports on Public Health and Medical Subjects No. 54, Ministry of Health; 1929. p. 1–27; London, England.
51. Faber WM. The nasal mucosa and the subarachnoid space. Am J Anat. 1937;62(1):121–148.
52. Yoffey JM, Drinker CK. Some observations on the lymphatics of the nasal mucous membrane in the cat and monkey. J Anat. 1939;74(Pt 1):45–52.3.
53. Schlosser RJ, Wilensky EM, Grady MS, Bolger WE. Elevated intracranial pressures in spontaneous cerebrospinal fluid leaks. Am J Rhinol. 2003;17(4):191–195.
54. Smalley ZS, Venable GT, Einhaus S, Klimo P Jr. Low-pressure hydrocephalus in children: a case series and review of the literature. Neurosurgery. 2017;80(3):439–447.
55. Erlich SS, McComb JG, Hyman S, Weiss MH. Ultrastructural morphology of the olfactory pathway for cerebrospinal fluid drainage in the rabbit. J Neurosurg. 1986;64(3):466–473.
56. Kincaid AE, Hudson KF, Richey MW, Bartz JC. Rapid transepithelial transport of prions following inhalation. J Virol. 2012;86(23):12731–12740.
57. Kincaid AE, Ayers JI, Bartz JC. Specificity, size, and frequency of spaces that characterize the mechanism of bulk transepithelial transport of prions in the nasal cavities of hamsters and mice. J Virol. 2016;90(18):8293–8301.